



Cite this: DOI: 10.1039/d5lc00978b

## Development of a nasal airway-on-chip co-culture model to study particulate matter exposure

 Amanda C. Walls,<sup>a</sup> Adrienne S. Vaughan<sup>a</sup> and Kartik Balachandran \*<sup>ab</sup>

Particulate matter (PM) is a major component of urban air pollution and is strongly associated with respiratory diseases. However, the mechanisms of PM-induced inflammation remain poorly understood due to a lack of physiologically-relevant airway models which can incorporate PM exposure. To address this, we used our nasal airway-on-chip platform to establish a co-culture model of human nasal epithelial cells and human pulmonary microvascular endothelial cells and used this model to investigate the effects of PM exposure on the nasal airway. In particular, we sought to understand the PM-induced reactive oxygen species (ROS)-mediated inflammatory response of the co-culture. Upon PM exposure, we observed a significant increase in ROS production consistent with oxidative stress-mediated injury. Additionally, treatment with the ROS scavenger *N*-acetyl-cysteine attenuated ROS levels and showed a trend toward reduced inflammation, suggesting a protective effect. These findings support the utility of our model for studying PM-induced airway inflammation in a more physiologically-relevant environment.

 Received 17th October 2025,  
 Accepted 3rd March 2026

DOI: 10.1039/d5lc00978b

[rsc.li/loc](http://rsc.li/loc)

### 1. Introduction

Air pollution has recently become a critical global public health issue, with the World Health Organization estimating that 4.2 million deaths occur annually because of harmful particulate matter (PM) exposure.<sup>1,2</sup> This problem is exacerbated in urban regions.<sup>2,3</sup> PM is derived from a wide range of sources including vehicle emissions, industrial activities, waste combustion, and agricultural processes. These particles contain harmful chemical and biological components such as sulfates, nitrates, heavy metals, polycyclic aromatic hydrocarbons (PAHs), and allergens. Particulate matter is typically classified by aerodynamic diameter into PM<sub>10</sub> (particles  $\leq 10 \mu\text{m}$ ) and PM<sub>2.5</sub> (particles  $\leq 2.5 \mu\text{m}$ ). Larger particles primarily deposit in the upper respiratory tract, whereas finer particles can reach the lower airways and alveolar regions.<sup>3</sup> Chronic exposure to PM is linked to a broad spectrum of respiratory diseases, including asthma, lung cancer, and chronic rhinitis.<sup>4–6</sup>

The nasal mucosa serves as the primary interface between inhaled air and the respiratory tract, acting as a critical barrier against airborne pollutants and pathogens. The nasal epithelium is composed of ciliated and non-ciliated epithelial cells, along with mucus-secreting goblet cells. Mucus traps inhaled particles, and cilia beat to move the contaminated mucus out of the airway. Beneath the

epithelium, endothelial cells help regulate inflammation and immune responses.

Exposure to PM has been shown to initiate a cascade of pathological events in the airway epithelium and endothelium, leading to barrier dysfunction, increased pro-inflammatory cytokine release, excessive mucus production, and impaired mucociliary clearance.<sup>7,8</sup> Despite growing evidence linking PM to airway injury, the underlying cellular and molecular mechanisms remain poorly understood. One possible mechanism involves the generation of reactive oxygen species (ROS), which can disrupt cell membranes, damage intracellular organelles, and initiate an oxidative stress response.<sup>9</sup> Oxidative stress results from an imbalance between ROS production and antioxidant defenses, and can activate intracellular signaling pathways, such as mitogen activated protein kinase-nuclear factor (MAPK-NF- $\kappa$ B), leading to an increase in inflammatory cytokines and further tissue injury. Some studies using both *in vivo* and *in vitro* models have reported increased inflammatory markers following PM exposure, and have shown these effects to be mitigated by treatment with *N*-acetyl-cysteine (NAC), which is a known antioxidant and ROS-scavenger.<sup>8,9</sup> These results suggest a robust inflammatory response mediated by oxidative stress.

Although some studies have been conducted to understand the effects of PM across various portions of the respiratory tract, the nasal airway remains an under-researched area. This research gap likely exists because there are very few models which can accurately recapitulate the nasal airway and incorporate particulate matter exposure simultaneously.<sup>10–12</sup> Recent studies have investigated the role

<sup>a</sup> Department of Biomedical Engineering, University of Arkansas, Fayetteville, AR, USA. E-mail: kbalacha@uark.edu; Tel: +1 479 575 3376

<sup>b</sup> Humimic Biosystems, Fayetteville, AR, USA



of PM in lung and nasal epithelial cell cultures, but these are often performed under static, submerged conditions with cells that have not been differentiated at the air-liquid interface (ALI). Additionally, while it is well-understood that endothelial cells play a pivotal role in modulating inflammatory responses, few models have incorporated endothelial cells when investigating PM-induced inflammation. In order to elucidate the role of ROS in PM-induced nasal airway inflammation, a nasal airway model which can more accurately recapitulate the native airway environment during PM exposure is needed.

We have previously reported the development of a nasal airway-on-chip platform which can sustain nasal epithelial cell culture for 21 days at the ALI and has the capability to incorporate physiological breathing.<sup>13</sup> In this study, we sought to further advance the physiological relevance of the platform by establishing a co-culture with microvascular endothelial cells. Additionally, we sought to validate the ability of the nasal airway-on-chip to support PM exposure. We used our advanced model to investigate PM-induced airway responses, with an emphasis on ROS-mediated inflammatory mechanisms.

## 2. Materials and methods

### 2.1. Preparation of the nasal airway-on-chip

The overall design of the nasal airway-on-chip consists of an air channel and media chamber separated by a porous polycarbonate membrane, with inlet and outlet ports for media changes (Fig. 1a). Each end of the airway chamber is

tapered in order to connect to an external flow system. To make the polydimethylsiloxane (PDMS) media chambers, a mold was 3D printed from polylactic acid (PLA) plastic and filled with Sylgard 184 PDMS (Dow Corning) and allowed to cure at 40 °C for 24 hours (Fig. 1b). Once removed from molds, polypropylene fittings (Cole-Parmer) were attached for media exchange ports using fresh PDMS and curing under a 50 g weight at 40 °C for 24 hours. To attach the completed media chambers to the chip, a ultraviolet (UV) plasma gun was used to functionalize both the chip and PDMS surfaces. Fresh PDMS was then used to attach and seal the media chambers. All other portions of the chip were constructed as described in previously. Chips were rinsed with de-ionized (DI) water and sterilized in ethylene oxide gas before use.

### 2.2. Cell culture and determination of appropriate co-culture media conditions

Primary human pulmonary microvascular endothelial cells (hPMECs; PromoCell) were expanded in flasks using complete endothelial cell medium (Cell Biologics). Media was changed every 1 to 2 days and cells were passaged to new flasks once 70–90% confluent using 0.05% trypsin-ethylenediaminetetraacetic acid (EDTA) (Cell Biologics). HPMECs were used for experiments in passages 5–7. For co-culture experiments, hPMECs were seeded onto polycarbonate membranes coated with rat tail Collagen I at  $7 \mu\text{g cm}^{-2}$  (Corning) at a density of 50 000 cells per  $\text{cm}^2$  on transwells (Nunc<sup>TM</sup>) and in the nasal chip. For transwell experiments, transwells were flipped upside down so hPMECs could be seeded on the basal side. For chips, cells were seeded into the media chamber and the chip was oriented so that cells could attach to the membrane. After 6 hours, transwells and chips were flipped to their regular orientations and media was added to the basal and apical sides. HPMECs were cultured for 24 hours before epithelial cells were added to the co-culture.

Primary human nasal epithelial cells (hNECs) from both a commercial source (PromoCell) and nasal swab isolations (Institutional Approval Number: 2301444696) were expanded to passage 2 in flasks until 70% confluent using PneumaCult-Ex airway epithelial cell media (StemCell Technologies) 48.<sup>13,14</sup> Animal Component-Free Dissociation Kit (StemCell Technologies) was used for passaging. HNECs in passage 3 were seeded onto apical transwell side at a density of 250 000 cells per  $\text{cm}^2$  or the air channel side of chips at the same density of 250 000 cells per  $\text{cm}^2$ . Chips were oriented so that hNECs could adhere to the membrane. HNECs on transwells or chips were cultured for 24 hours, until 100% confluent, with PneumaCult-Ex airway epithelial cell media on the hNEC side of the polycarbonate membrane and complete endothelial cell medium on the hPMEC side. After confluency was reached, the ALI was established by removing media from the apical side of transwells or air channel of chips.

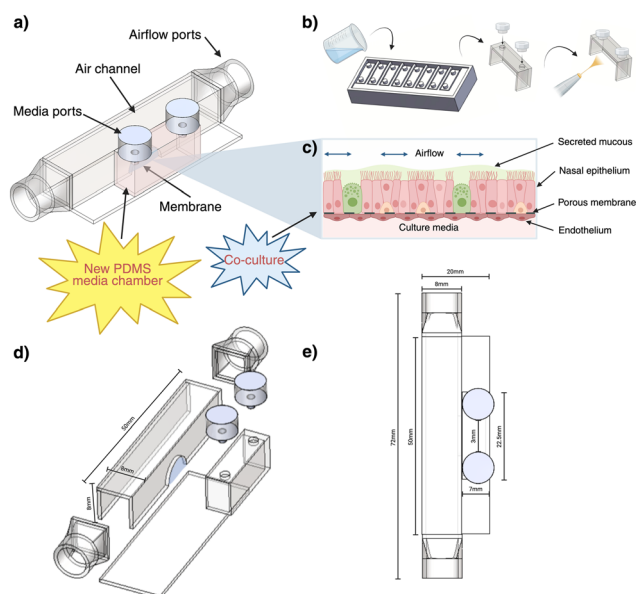


**Fig. 1** (a) Schematic of chip with new PDMS media chamber shown in red. (b) Workflow for fabricating PDMS media chambers *via* replica molding. (c) Schematic showing cellular organization on the nasal airway-on-chip platform. Pink = ciliated and non-ciliated epithelial cell, green = goblet cells, orange = basal cells, red = endothelial cells. (d) Exploded view of nasal airway-on-chip platform. (e) Top view of nasal airway-on-chip diagram. Created with <https://BioRender.com>.



Based on previous reports, at least 14 to 21 days of culture at the ALI is required for the maturation of the hNEC epithelium into a pseudostratified structure with both ciliated and goblet cells.<sup>15–17</sup> To validate these published reports, hNECs were cultured on polycarbonate membranes for either 14 or 21 days. Immunocytochemistry (ICC), as outlined in section 2.5.1, was used to identify cilia (acetylated- $\alpha$ -tubulin) and goblet cells (MUC5AC). Trans-endothelial electrical resistance (TEER) was also measured from the day that ALI was initiated, every two to three days until day 21 as outlined in section 2.5.2.

To determine the best media composition for co-culture, media on the basal side of transwells was replaced with either ALI+ media (PneumaCult-ALI airway epithelial cell media (StemCell Technologies) supplemented with 0.1% EGF and 0.1% VEGF from the endothelial medium kit (Cell Biologics)), or 1:1 media (50% PneumaCult-ALI media with 50% complete endothelial cell media).

For all experiments, media was changed every two days. After day 7 of ALI culture, hNECs were washed with PBS during each media change to remove excess mucous. After day 14 of ALI culture, chip samples were preconditioned with airflow as outlined in our previous work.<sup>13</sup> Co-cultures were sustained for a total of 21 days at the ALI before experiments followed by analyses. Based on the results of the media composition experiments, 1:1 media was used for all other experiments. A representative timeline of the cell culture process, including airflow pre-conditioning and PM exposure is shown in Fig. 2.

### 2.3. Pre-conditioning airflow setup

Prior to PM exposure, chips were exposed to pre-conditioning flow similar to what we have previously reported.<sup>13</sup> Briefly, a mass flow controller (Alicat Scientific) was connected to a dried, filtered, compressed air source and a vacuum pump. An in-line humidifier (Medicomp) was placed at the outlet of the controller just before the chip connection. The flow experiments were run in the cell culture incubator at 37 °C, 95% humidity, and 5% CO<sub>2</sub>. The mass flow controller was programmed to create bi-directional flow in the chip by inputting the sine wave function. A flow condition resulting

in a wall shear stress of 0.05 dyne per cm<sup>2</sup> was used to pre-condition chips. To achieve this condition, the mass flow rate was set to 0.85 standard liters per minute (SLPM) at a breathing rate of 12 cycles per minute.

### 2.4. PM exposure experiments

PM 1648a was purchased from NIST and resuspended in sterile PBS to make a 10 $\times$  stock solution (168 mg mL<sup>-1</sup>). A 1 $\times$  solution was made to deposit on the membrane surface by diluting the 10 $\times$  solution in 1:1 cell culture media. Immediately prior to dilution or deposition on the membrane, the PM suspensions were vortexed to ensure even distribution of PM. A 10  $\mu$ L volume of 1 $\times$  PM solution was deposited onto the hNEC side of membranes for a final concentration of 300  $\mu$ g cm<sup>-2</sup>. This small volume allowed the media to evaporate quickly to ensure the ALI was still well-established during PM exposure.

Chips were divided into three different treatment groups shown in Table 1: control, +PM, and +PM +NAC. Chips in the control group were exposed to 10  $\mu$ L of 1:1 media on the hNEC side of the membrane, +PM chips were exposed to 10  $\mu$ L of the 1 $\times$  PM solution on the hNEC side of the membrane, and chips in the +PM +NAC group were exposed to 5 mM NAC (Sigma) on the hNEC side of the membrane for 30 minutes immediately before PM exposure, then NAC was removed and 10  $\mu$ L of the 1 $\times$  PM solution was deposited. To make the NAC solution, NAC was first dissolved in PBS to make a 100 mM stock solution. A 5 mM solution was made by diluting the 100 mM stock in 1:1 media, and a 400  $\mu$ L volume was added to the air channel of the chip for NAC treatment. Chips were subjected to 48 hours of control or PM exposure before analyses were conducted.

### 2.5. Endpoint assays

**2.5.1. Immunocytochemistry.** Cells on polycarbonate membranes were fixed in 4% paraformaldehyde for 12 minutes and subsequently washed with PBS for 10 minutes. Cells were blocked and permeabilized simultaneously at room temperature for 1 hour using a solution of PBS with normal serums (final concentration: 2%, Sigma), bovine serum albumin (final concentration: 1%, Sigma), cold fish skin gelatin (CFSG, final concentration: 0.1%, Sigma), Triton X-100 (final concentration: 0.1%, Sigma), and Tween-20 (final concentration: 0.05%, Amresco). Cells were washed three times and primary antibody solution (PBS with BSA 1%, CFSG 0.1%) was added and incubated overnight at 4 °C. Primary antibodies were anti-MUC5AC (1:800, mouse, Invitrogen 45 M1), anti-acetylated- $\alpha$ -tubulin (1:800, mouse, Sigma-Aldrich T7451), anti-ZO-1 (1:100, rabbit, Invitrogen 40-2200), and anti-vWF (1:100, mouse, Invitrogen MA5-14029). After primary incubation, cells were washed three times and incubated for 2 hours at room temperature in secondary antibody solutions: Alexa Fluor 488 donkey anti-mouse (1:100, Invitrogen A21202) and Alexa Fluor 594 donkey anti-rabbit (1:100, Invitrogen A32754) and DAPI (1:500, Invitrogen D1306) as a nuclear

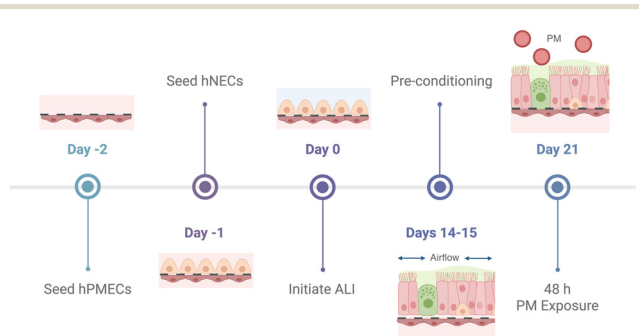


Fig. 2 Representative timeline of cell seeding through to PM exposure on the nasal airway-on-chip. Created with <https://BioRender.com>.



**Table 1** Experimental treatment groups for PM exposure

Control	+PM	+PM +NAC
10 $\mu\text{L}$ media for 48 h (vehicle control)	300 $\mu\text{g cm}^{-3}$ PM in 10 $\mu\text{L}$ media for 48 h	5 mM NAC for 30 min + 300 $\mu\text{g cm}^{-3}$ PM in 10 $\mu\text{L}$ media for 48 h

counterstain. Cells were imaged using an Olympus IX83 inverted confocal microscope.

**2.5.2. Transepithelial electrical resistance (TEER).** Transepithelial electrical resistance (TEER) was measured on transwells using an EVOM 2 instrument with accompanying chopstick electrodes (World Precision Instruments). TEER on chips was measured using a custom-built, Arduino-based TEER measurement system 65. Prior to cell seeding on chips, blank pre-warmed media was added to the air channel and media chambers and blank TEER values were recorded for each chip. For measurements at the ALI, pre-warmed media was added to the air channel to cover the membrane and electrodes were inserted into the air channel and media chamber for readings. TEER values were measured on day 0 (directly before ALI initiation), days 1, 7, 14, and 21 of ALI culture, and again directly following 48 hours of PM exposure. All values were subtracted from the average blank reading of chips and normalized to the membrane area.

**2.5.3. Assessment of cell viability.** An MTS assay (Abcam) was used to determine the metabolic activity of the cells after PM exposure. Media was removed from the media chamber and replaced with 300  $\mu\text{L}$  of MTS solution. Chips were oriented so that the MTS solution was covering the membrane and incubated for 2 hours. Then, 200  $\mu\text{L}$  of MTS solution was collected from each chip and absorbance was measured using a Biotek Synergy plate reader (Biotek).

**2.5.4. Detection of reactive oxygen species (ROS).** To detect the production of ROS in chips, a de-acetylated 2',7'-dichlorodihydrofluorescein (H2DCF) based assay kit (*In Vitro* ROS Assay, Cell Biolabs Inc.) was used to measure the ROS concentration present in media supernatant. Media was refreshed immediately prior to PM exposure and was collected after PM exposure ( $n = 4$  for each treatment) and stored at  $-80^\circ\text{C}$  until analyses were performed. The ROS concentration of samples were determined based on a hydrogen peroxide standard curve.

**2.5.5. MUC5AC secretion.** To analyze MUC5AC secretions, hNECs were washed 24 hours before PM experiments to remove any mucus. Immediately before PM exposure, hNECs were incubated with 400  $\mu\text{L}$  of PBS for 15 minutes. Mucus samples ( $n = 4$  for each treatment) were collected to establish a 24-hour baseline MUC5AC protein concentration. Immediately following PM exposure, hNECs were incubated with 400  $\mu\text{L}$  of PBS for 15 minutes and mucus was collected again. All samples were stored at  $-80^\circ\text{C}$  until the assay was performed. Mucus samples were analyzed for MUC5AC protein concentrations using an ELISA kit (NOVUS Biologicals, NBP2-76703) and normalized to the total protein concentrations in each sample. The percentage difference

between pre- and post-flow MUC5AC concentration was determined for each chip.

**2.5.6. Analysis of inflammation.** Secreted IL-8 and soluble ICAM-1 (sICAM-1) concentrations in media supernatants were analyzed to understand the inflammatory response of the co-culture to PM exposure. Fresh media was added to chips immediately before PM exposure, then the media was collected immediately following PM exposure. All samples were stored at  $-20^\circ\text{C}$  until the assay was performed. Media samples ( $n = 4$  for each treatment) were analyzed for IL-8 and sICAM-1 using ELISA kits (Invitrogen, Biotechne). Analyte concentrations were normalized to total protein concentrations.

**2.5.7. Statistical analysis.** Statistical testing and data plotting were performed using GraphPad Prism statistics software. All error bars in figures are represented as the mean  $\pm$  standard error of the mean (SEM) and significance was determined using a one-way ANOVA with Tukey's *post hoc* test. Significance was set as  $p \leq 0.05$  for each test and is demonstrated as \* for  $p \leq 0.05$ , and \*\* for  $p \leq 0.01$ .

## 3. Results

### 3.1. Appropriate duration for ALI maturation

To characterize the differentiation of the cultured nasal epithelium, we performed ICC staining of cilia (acetylated- $\alpha$ -tubulin) and goblet cells (MUC5AC) at days 14 and 21 of ALI

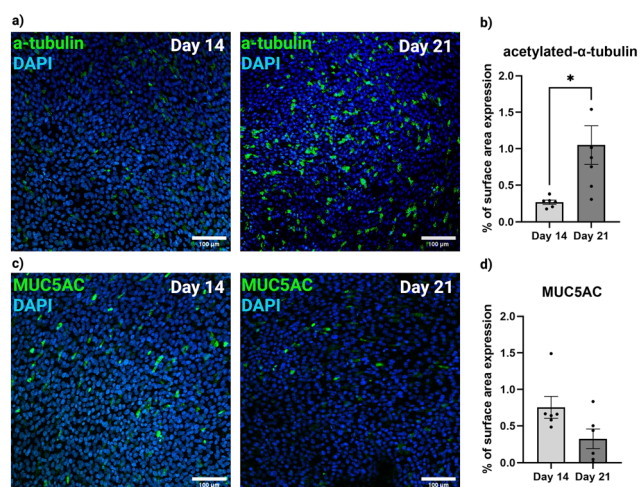


**Fig. 3** (a) hNECs stained for acetylated- $\alpha$ -tubulin (green) and DAPI (blue). (b) Plot of percent area coverage of acetylated- $\alpha$ -tubulin immunopositive cells. (c) hNECs stained for MUC5AC (green) and DAPI (blue). (d) Plot of percent area coverage of MUC5AC immunopositive cells. Scale bars are all 100  $\mu\text{m}$ .



and analyzed the images to determine the relative abundance of each cell type by surface area. Fig. 3 shows that the expression of acetylated- $\alpha$ -tubulin significantly increases ( $p = 0.0212$ ) from days 14 to 21, indicating that cells at day 21 of ALI are more well-differentiated and experiments and analyses should likely be performed no earlier. There was no significant difference ( $p = 0.0580$ ) found in the expression of MUC5AC from days 14 to 21.

TEER can be measured to assess the integrity of the epithelial monolayer. Higher resistance values indicate that cells are fully confluent on the membrane and are expressing tight junction proteins to keep the monolayer intact. As seen in Fig. 4, the TEER values show a steep increase during the first few days of culture at the ALI, peaking at around 12 days before reducing and stabilizing between day 14 and day 21 of ALI culture.

### 3.2. Sustained ALI co-culture of hNECs and hPMECs

We next sought to validate the co-culture of epithelial and endothelial cells at the ALI for 21 days. HPMECs were seeded on the basal side of polycarbonate membranes, and once attached for 24 hours, hNECs were seeded on the apical side. Once both cell types were fully confluent (about 24 hours after seeding hNECs), the ALI was established by removing media from the apical side of the membrane and adding either ALI+ or 1:1 media to the basal side. After 21 days of ALI culture, epithelial cells were analyzed for goblet (MUC5AC) and ciliated (acetylated- $\alpha$ -tubulin) cell expression. The ICC images in Fig. 5(a and b) showed confluent monolayers in both the ALI+ and 1:1 media groups, and no differences in cilia expression were observed; however, less MUC5AC expression was observed in the ALI+ media group, indicating a lower number of goblet cell differentiation.

Additionally, ZO-1 staining of hPMECs (Fig. 5(c)) showed that endothelial cells in the ALI+ group had begun to detach from the membrane and no longer showed a confluent monolayer. HPMECs in the 1:1 media group showed a more

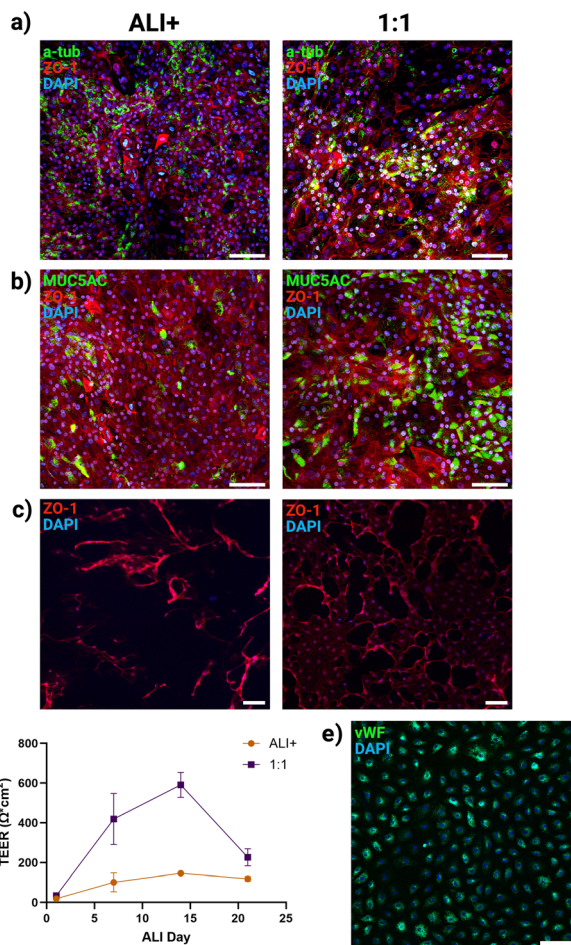


Fig. 5 (a) HNECs stained for acetylated- $\alpha$ -tubulin (green). (b) HNECs stained for MUC5AC (green). HNECs (a and b) and hPMECs (c) are also stained for ZO-1 (red) and DAPI (blue) for both ALI+ (left) and 1:1 (right) media. (d) TEER values over 21 days of ALI culture for co-cultures in ALI+ and 1:1 media. (e) hPMECs in 1:1 media stained for vWF (green) and DAPI (blue). Scale bars are all 100  $\mu\text{m}$ .

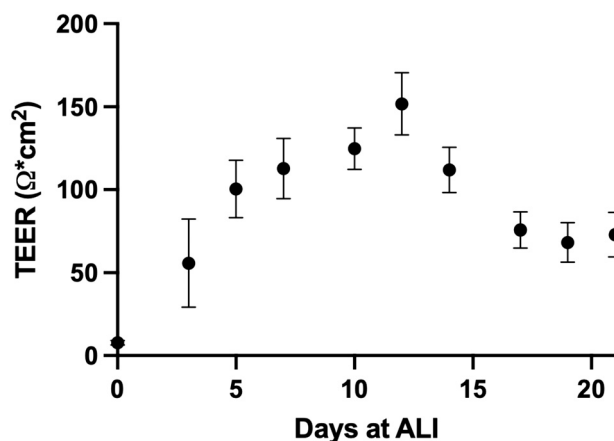


Fig. 4 Longitudinal TEER measurements on hNECs cultured on polycarbonate membranes.

intact monolayer. These results were confirmed by TEER measurements, shown in Fig. 5(d), which showed significantly decreased resistance values in the ALI+ media compared to the 1:1 media. HPMECs in the 1:1 media group were further characterized and showed expression of the endothelial cell marker vWF (Fig. 5(e)), confirming that endothelial cells could be sustained at the ALI for 21 days.

Taken together, these results indicate that ALI+ media was likely sufficient for hNECs, but was insufficient for prolonged hPMEC culture. We conclude that the 1:1 media is capable of producing well-differentiated hNECs and can sustain healthy hPMECs throughout 21 days of ALI culture. All following experiments were carried out using the 1:1 media.

### 3.3. Cell viability and barrier integrity post-PM exposure

PM exposure has previously been shown to affect cell viability and metabolism as well as barrier integrity of cell monolayers.<sup>8,9</sup> For PM exposure experiments on chips, we



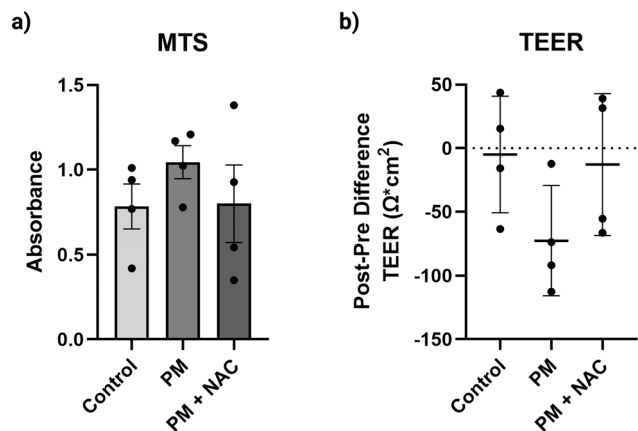


Fig. 6 (a) MTS absorbance readings. (b) Difference in pre- and post-PM exposure TEER values.

measured cell viability using an MTS assay and found that there were no significant differences between in viability between groups (Fig. 6(a)). This was an expected result as we chose a PM exposure concentration previously shown to have few cytotoxic effects.<sup>8,9</sup> We also characterized barrier integrity by comparing TEER measurements before and after the 48 hour PM exposure (Fig. 6(b)). The results indicate a decrease in TEER, and thus a decrease in barrier integrity, following PM exposure, when comparing post- and pre-exposure TEER. Although the mean TEER value difference appeared lower for the PM group ( $-72.55 \pm 43.27 \Omega \text{ cm}^2$ ) compared to both control ( $-4.95 \pm 45.83 \Omega \text{ cm}^2$ ) and NAC ( $-12.75 \pm 55.74 \Omega \text{ cm}^2$ ) groups, no statistical significance was observed ( $p = 0.18$  and  $p = 0.24$ , respectively); however, our results showed that all TEER values decreased for the PM-only exposed group.

### 3.4. PM-induced ROS production

PM can trigger the production of ROS in both epithelial and endothelial cells, which then leads to a cascade of inflammation.<sup>9</sup> In this study, we measured the ROS present in media supernatant after 48 hours of PM exposure. As shown in Fig. 7, we found that the concentration of ROS was significantly increased with PM exposure, both with and without the NAC treatment, compared to the control ( $p < 0.0001$ ). The NAC treatment produced a significantly lower average ROS concentration ( $2.985 \pm 0.246 \mu\text{M}$ ) compared to PM exposure with no NAC treatment ( $3.513 \pm 0.331 \mu\text{M}$ ;  $p = 0.0385$ ).

### 3.5. Changes in mucus production

MUC5AC is one of the most abundant mucin proteins produced by nasal epithelial cells and has been shown to have increased expression in the airway after exposure to PM.<sup>11</sup> We present mucus secretions of cells exposed to control, PM, and PM + NAC treatments in Fig. 8. Results are expressed as a percentage of the 24-hour baseline secretion for each chip. Cells exposed to PM + NAC produced significantly more mucus compared to both the control and PM-only treatment ( $p = 0.0015$  and  $p = 0.0191$ , respectively).

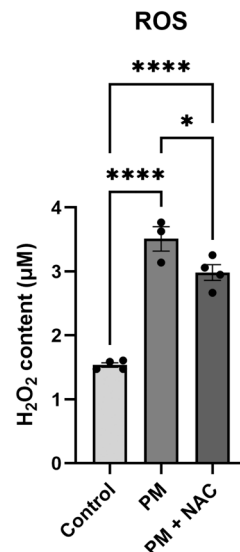


Fig. 7 ROS concentration in media supernatant after 48 hours of PM exposure. \*  $p < 0.05$ . \*\*\*\*  $p < 0.001$ .

There was no significant difference in mucus production between the control and PM-only groups ( $p = 0.2386$ ).

### 3.6. Changes in inflammatory response

To characterize the inflammatory response of cells to PM exposure and NAC treatment, we analyzed the concentration of IL-8, as well as the concentration of soluble ICAM-1 in media supernatant. IL-8 is a pro-inflammatory cytokine produced by both epithelial and endothelial cells and is commonly used to assess airway inflammation.<sup>9,11</sup> ICAM-1, a protein expressed on the surface of endothelial cells that promotes leukocyte adhesion and migration, has been shown to increase as a result of PM exposure.<sup>11</sup> The soluble form (sICAM-1) can be detected in media. As shown in Fig. 9(a), there was a trend toward increased IL-8 concentration in the

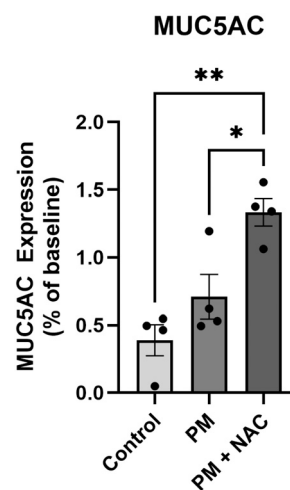


Fig. 8 Mucus production represented as a percentage of the 24-hour baseline. \*  $p < 0.05$ . \*\*  $p < 0.01$ .



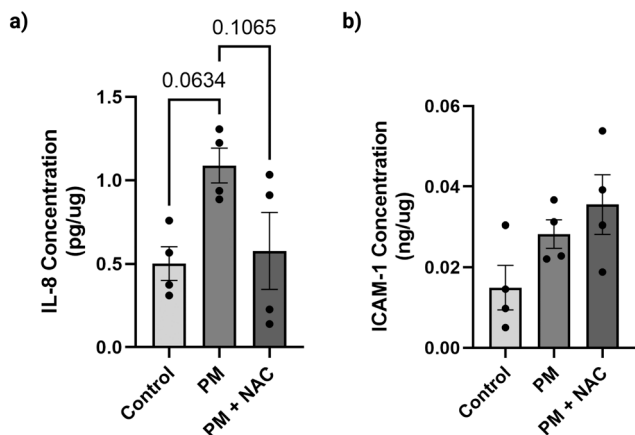


Fig. 9 (a) IL-8 concentration normalized to total protein concentration ( $\text{pg } \mu\text{g}^{-1}$ ) and (b) sICAM-1 concentration normalized to total protein concentration ( $\text{ng } \mu\text{g}^{-1}$ ) present in media supernatant after 48 hours of PM exposure.

PM group compared to the control ( $p = 0.0634$ ). Additionally, there was a trend toward decreased IL-8 concentration in the NAC-treated group ( $p = 0.1065$ ). There did not appear to be any significant differences between the sICAM-1 concentrations between treatment groups ( $p = 0.52$ ) (Fig. 9(b)).

## 4. Discussion

In this study, we have adapted our previously developed nasal airway-on-chip platform to sustain the co-culture of primary hNECs and hPMECs at the ALI.<sup>13</sup> Previous studies have typically cultured cells at the ALI for at least 14, 21 days, or even 30 days prior to any experimental analyses.<sup>15–17</sup> Another study reported that ALI cultures are suitable for prolonged experiments for 40 or more days *in vitro*.<sup>14</sup> However, the normal turnover rate of cilia *in vivo* is about 3 weeks.<sup>18</sup> Taken together, we expected the epithelial layer to be well-differentiated after 21 days, and we have demonstrated so in our results.

In our initial testing, we discovered that the original, fully-acrylic design of the platform was not conducive to sustained culture of hPMECs in the media chamber (Fig. S1), and we speculated that this was due to the poor oxygen permeability of acrylic (<1 barrer).<sup>19,20</sup> This is especially detrimental to airway epithelial and endothelial cells, which have one of the highest oxygen requirements of any cell type. PDMS is a common material used in organ-on-chip devices and has a significantly higher oxygen permeability coefficient (>700 barrer),<sup>19,20</sup> so we adapted the chip design to replace the acrylic media chamber with a PDMS media chamber. This adaptation allowed for the culture of endothelial cells in the media compartment, creating a functional platform for co-culture studies.

Previous studies have utilized differing media compositions for the co-culture of airway epithelial and endothelial cells, with some being used for short-term, non-ALI cultures and others for long-term ALI cultures.<sup>11,21</sup> In

establishing our own co-culture model of hNECs and hPMECs, we tested two different media compositions to determine what would best support long-term ALI culture. We tested 1) PneumaCult ALI media supplemented with 0.1% EGF and 0.1% VEGF (ALI+) and 2) a 1:1 combination of PneumaCult ALI media with Complete Endothelial Media (1:1). We reported that both the ALI+ and 1:1 media produced a well-differentiated epithelium similar to what we have observed in our previous work.<sup>13</sup> However, the endothelial cells did not appear to remain attached or viable across 21 days of ALI culture in the ALI+ media, with TEER measurements and ICC images confirming these results. The endothelial cells remained attached and expressed vWF after 21 days in the 1:1 media. We therefore concluded that the 1:1 media composition was suitable for our co-culture, and all subsequent studies were performed with this composition.

Once initial validations of the nasal airway co-culture were complete, we sought to test the effects of PM exposure with an emphasis on observing the ROS-mediated inflammation pathway. We exposed co-cultures on chips to PM for 48 hours, with some chips receiving a pre-treatment of NAC. Previous studies have reported that NAC can significantly attenuate the inflammatory effects of PM. A previous study showed that mice treated with NAC prior to PM exposure showed reduced inflammatory cytokine levels (IL1- $\beta$ , IL-6, IL-8, MMP-9) and reduced neutrophil and macrophage cell numbers compared to untreated mice.<sup>9</sup> Another study reported that NAC pre-treatment reduced the PM-induced stress response of endoplasmic reticulum in hNECs.<sup>8</sup> Our results showed that ROS concentrations in media were significantly increased following PM exposure, indicating that our urban PM source (PM 1648a) was capable of initiating oxidative stress in the co-culture model. Furthermore, we found that ROS concentrations significantly decreased with the 30 minute NAC pre-treatment, indicating that NAC was an effective ROS scavenger in our model.

Although we saw significant changes in ROS production with PM exposure and NAC treatment, PM did not significantly affect cell viability, barrier integrity, or inflammatory responses, though some trends were observed. Cell viability was characterized with an MTS assay, which has previously been used to determine the metabolic activity of respiratory cells such as human bronchial cells.<sup>22</sup> In the presence of living and metabolically active cells, phenazine methosulfate in the MTS reagent can be bio-reduced by NADPH-dependent dehydrogenase enzymes, which results in a colorimetric change that can be measured with a plate reader. A previous study reported that oxidative stress in airway cells resulted in decreased metabolic activity,<sup>22</sup> however, we did not see similar results in our PM-exposed chips. To analyze barrier integrity, we measured TEER. The average TEER value appeared to be lower for PM-exposed chips compared to control and NAC treated chips. Another study reported that mRNA expression of tight junction



proteins in airway epithelial cells was significantly decreased with PM exposure, which supports the trends we observed.<sup>23</sup>

We also found that PM exposure resulted in a trend toward significantly higher IL-8 secretions as collected on the endothelial side of our platform, but no significant differences in sICAM-1 were seen. Several previous studies have reported an increase in the mRNA expression of IL-8 with 24- and 48-hour PM exposures, as well as attenuated secretions with NAC treatment. The same trends have been observed with the mRNA expression of ICAM-1. As far as sICAM-1 is concerned, previous *in vitro* studies have reported the inhibitory effects of NAC on sICAM-1 on airway epithelial and endothelial cells cultured separately (not in co-culture).<sup>24,25</sup> A systematic review of clinical studies showed that oral or intravenous NAC administration did not result in significant changes in sICAM-1 level in patients.<sup>26</sup> Taken these prior studies in the context of our work, we see our microphysiological nasal-chip model mimicking more of the *in vivo* condition, where the co-culture of epithelial and endothelial cells may have had a moderating effect on ICAM-1 secretion in response to NAC administration. To our knowledge, ours is the first *in vitro* study where the effects of NAC treatment are studied on a nasal co-culture under physiological breathing conditions. It is possible that in such a co-culture model, that more time may be needed for significant inflammatory responses to be seen in protein expression but may show sooner when looking at transcriptional analyses. We believe that our model may have the ability to show more robust inflammatory and metabolic responses if PM exposure were lengthened.

We also analyzed mucus production in response to PM exposure. We report that mucus secretions were significantly higher with NAC treatment compared to both the control and PM-exposed groups. This finding contradicts several previous studies which propose NAC as an effective treatment for mucus hypersecretion, particularly in cases of COPD where mucus is thick and viscous.<sup>27–29</sup> Additionally, PM exposure has been shown to increase the mucus production of nasal mucosa in mice, which further contradicts our findings.<sup>30</sup> It should be noted that the viscoelastic properties of mucus can be altered during oxidative stress to produce thicker and more viscous mucus.<sup>31</sup> NAC is known to act on viscous mucus by hydrolyzing the disulfide bonds of mucus proteins to reduce its overall viscosity and facilitate its clearance from the airway.<sup>27</sup> Taking all of this together, we suggest that our method of mucus collection may present a potential explanation for the observed increase in mucus concentration with the NAC treatment. In order to collect mucus from the epithelial surface, we incubate the hNEC side of the membrane in PBS for 15 minutes, which allows for the mucus to be dissolved and collected into the PBS. No vigorous washing or scraping of the cell surface occurs, so the collected mucus comes only from what is dissolved during the incubation. Therefore, it is possible that thicker mucus was not fully dissolved and collected, while thinner, less viscous mucus is dissolved more readily, leading to our

observed discrepancies. Since NAC is well known to decrease mucus viscosity, this could likely explain why more mucus was measured in the NAC treated samples. In order to fully understand this phenomenon, future studies should aim to evaluate the viscoelastic properties of mucus samples. Other methods of mucus collection and measurement could also be explored.

## Conclusions

Overall, we have developed and validated a novel nasal airway-on-chip co-culture model which can support the sustained ALI culture of hNECs and hPMECs. We were able to expose this nasal airway model to PM and reported significant PM-induced, ROS-mediated physiological responses. We observed altered inflammatory responses to PM exposure that were reduced by NAC treatment. Our results emphasize the utility of our model for future PM exposure studies on the nasal mucosa.

## Author contributions

Amanda Walls: conceptualization, investigation, data curation, formal analysis, writing – original draft, writing – review & editing. Adrienne Vaughan: investigation, writing – review & editing. Kartik Balachandran: conceptualization, methodology, validation, writing – review & editing, supervision, project administration, funding acquisition.

## Conflicts of interest

Corresponding author, Kartik Balachandran is cofounder and CTO of Humimic Biosystems LLC, a company developing organ-on-chip platforms. The research presented in this manuscript was conducted at the University of Arkansas and supports the future commercialization of this platform with Humimic Biosystems LLC. The authors declare this potential conflict of interest and affirm that the research was conducted objectively and without commercial bias.

## Data availability

Quantitative data sets generated during the study are available as part of the supplementary information (SI).

Supplementary information is available. See DOI: <https://doi.org/10.1039/d5lc00978b>.

## Acknowledgements

This study was supported by the National Science Foundation Graduate Research Fellowship, the Arkansas Biosciences Institute, and the Department of Defense (Grant number: W81XWH2210174).

## References

- G. Shaddick, M. L. Thomas, P. Mudu, G. Ruggeri and S. Gummy, *npj Clim. Atmos. Sci.*, 2020, **3**, 23.



- 2 W. H. Organization, *et al.*, *Tydskr. Skoon Lug*, 2016, **26**, 6.
- 3 M. Guarnieri and J. R. Balmes, *Lancet*, 2014, **383**, 1581–1592.
- 4 S. Liu, Y. Zhou, S. Liu, X. Chen, W. Zou, D. Zhao, X. Li, J. Pu, L. Huang and J. Chen, *et al.*, *Thorax*, 2017, **72**, 788–795.
- 5 S. A. Weichenthal, E. Lavigne, G. J. Evans, K. J. Godri Pollitt and R. T. Burnett, *Am. J. Respir. Crit. Care Med.*, 2016, **194**, 577–586.
- 6 Y.-F. Xing, Y.-H. Xu, M.-H. Shi and Y.-X. Lian, *J. Thorac. Dis.*, 2016, **8**, E69.
- 7 C. Xu, M. Zhang, W. Chen, L. Jiang, C. Chen and J. Qin, *ACS Biomater. Sci. Eng.*, 2020, **6**, 3081–3090.
- 8 S. K. Park, S. H. Yeon, M.-R. Choi, S. H. Choi, S. B. Lee, K.-S. Rha and Y. M. Kim, *Am. J. Rhinol. Allergy*, 2021, **35**, 817–829.
- 9 J. Wang, J. Huang, L. Wang, C. Chen, D. Yang, M. Jin, C. Bai and Y. Song, *J. Thorac. Dis.*, 2017, **9**, 4398.
- 10 J. Shrestha, S. T. Ryan, O. Mills, S. Zhand, S. R. Bazaz, P. M. Hansbro, M. Ghadiri and M. E. Warkiani, *Biofabrication*, 2021, **13**, 035028.
- 11 J. Byun, B. Song, K. Lee, B. Kim, H. W. Hwang, M.-R. Ok, H. Jeon, K. Lee, S.-K. Baek and S.-H. Kim, *et al.*, *J. Biol. Eng.*, 2019, **13**, 88.
- 12 S. Elias-Kirma, A. Artzy-Schnirman, P. Das, M. Heller-Algazi, N. Korin and J. Sznitman, *Front. Bioeng. Biotechnol.*, 2020, **8**, 91.
- 13 A. C. Walls, M. van Vegchel, A. Lakey, H. Gauri, J. Dixon, L. A. Ferreira, I. Tandon and K. Balachandran, *Biofabrication*, 2024, **16**, 045021.
- 14 V. Manna and S. Caradonna, *STAR Protoc.*, 2021, **2**, 100782.
- 15 J. Jia, J. Xia, R. Zhang, Y. Bai, S. Liu, M. Dan, T. Li, T. Yan, L. Chen and S. Gong, *et al.*, *Chemosphere*, 2019, **233**, 309–318.
- 16 M.-K. Lee, J.-W. Yoo, H. Lin, Y.-S. Kim, D.-D. Kim, Y.-M. Choi, S.-K. Park, C.-H. Lee and H.-J. Roh, *Drug Delivery*, 2005, **12**, 305–311.
- 17 L. Müller, L. E. Brighton, J. L. Carson, W. A. Fischer and I. Jaspers, *et al.*, *J. Visualized Exp.*, 2013, 50646.
- 18 E. Heffler, M. Landi, C. Caruso, S. Fichera, F. Gani, G. Guida, M. Liuzzo, M. Pistorio, S. Pizzimenti and A. Riccio, *et al.*, *Clin. Exp. Allergy*, 2018, **48**, 1092–1106.
- 19 C. J. Ochs, J. Kasuya, A. Pavesi and R. D. Kamm, *Lab Chip*, 2014, **14**, 459–462.
- 20 T. Femmer, A. J. Kuehne and M. Wessling, *Lab Chip*, 2014, **14**, 2610–2613.
- 21 L. Si, H. Bai, M. Rodas, W. Cao, C. Y. Oh, A. Jiang, R. Moller, D. Hoagland, K. Oishi and S. Horiuchi, *et al.*, *Nat. Biomed. Eng.*, 2021, **5**, 815–829.
- 22 C. Y. Wong, H. X. Ong and D. Traini, *Life Sci.*, 2022, **298**, 120487.
- 23 Ł. Zaręba, K. Piszczatowska, K. Dżaman, K. Soroczynska, P. Motamedi, M. J. Szczepański and N. Ludwig, *J. Pers. Med.*, 2024, **14**, 98.
- 24 D. Radomska-Leśniewska, A. Sadowska, F. Van Overveld, U. Demkow, J. Zieliński and W. De Backer, *J. Physiol. Pharmacol.*, 2006, **57**, 325–334.
- 25 D. M. Radomska-Leśniewska, E. Skopińska-Różewska, E. Jankowska-Steifer, M. Sobiecka, A. M. Sadowska, A. Hevelke and J. Malejczyk, *Pharmacol. Rep.*, 2010, **62**, 131–138.
- 26 M. Mahmoudinezhad, Z. Ghavami, P. Jamilian, M. Zarezadeh and A. Ostadrahimi, *Clin. Nutr. Open Sci.*, 2023, **52**, 136–150.
- 27 S. Banerjee and S. McCormack, *Acetylcysteine for Patients Requiring Mucous Secretion Clearance: A Review of Clinical Effectiveness and Safety*, Canadian Agency for Drugs and Technologies in Health, Ottawa (ON), 2019.
- 28 P. Rogliani, G. M. Manzetti, S. Gholamalishahi, M. Cazzola and L. Calzetta, *Int. J. Chron. Obstruct. Pulmon. Dis.*, 2024, 2347–2360.
- 29 C. K. Rhee, S. Y. Lim, W.-Y. Lee, J. Y. Jung, Y. B. Park, C. Y. Lee, Y. I. Hwang, J. W. Song, W.-I. Choi and K. H. Yoo, *et al.*, *BMC Pulm. Med.*, 2024, **24**, 434.
- 30 W. Gu, T. Hou, H. Zhou, L. Zhu, W. Zhu and Y. Wang, *Int. Immunopharmacol.*, 2023, **115**, 109658.
- 31 M. Abrami, A. Biasin, F. Tescione, D. Tierno, B. Dapas, A. Carbone, G. Grassi, M. Conese, S. Di Gioia and D. Larobina, *et al.*, *Int. J. Mol. Sci.*, 2024, **25**, 1933.

